

# Mechanisms of CO<sub>2</sub> separation by microporous crystals estimated by computational chemistry

Y. Nakazaki <sup>a,\*</sup>, Y. Tanaka <sup>b</sup>, N. Goto <sup>b</sup>, T. Inui <sup>b</sup>

<sup>a</sup> Department of Industrial Chemistry, Osaka Prefectural College of Technology, Neyagawa, Osaka 572, Japan

<sup>b</sup> Division of Energy and Hydrocarbon Chemistry, Graduate School of Engineering, Kyoto University, Sakyo-ku, Kyoto 606-01, Japan

## Abstract

The diffusion and adsorption of CO<sub>2</sub> inside the pores of Li, Na, and K ion-exchanged X-type zeolites were simulated by molecular dynamics and Monte Carlo calculations. Carbon dioxide diffused inside the zeolites pores while it was colliding with pore walls. Then it stayed in a super cage of zeolites. Inside the pore of Li<sup>+</sup> ion-exchanged X-type zeolite (Li-X), the electrostatic potential term was  $-570$  kcal/mol, this value was considerably smaller than those of CO<sub>2</sub> inside the pores of Na-X and K-X. On the other hand, from Monte Carlo calculations, CO<sub>2</sub> was found to strongly absorb near the 3B site for Li<sup>+</sup> ions. When CO<sub>2</sub> passed through the pores of alkali ion-exchanged X-type zeolites, the interaction between the CO<sub>2</sub> molecule and the 3B site for Li cation was fairly large.

## 1. Introduction

Carbon dioxide accumulation could cause global warming, and it is, therefore, potentially one of the most serious environmental problems. Carbon dioxide from fossil fuel combustion in large facilities should be concentrated and/or separated from gas mixtures before submitting it to catalytic reaction. Pressure-swing adsorption (PSA) would be one of the most practical methods for the separations, and its efficiency depends on the performance of the adsorbent. Narrow-pore size zeolites are suitable adsorbents for this purpose [1,2]. For example, CaA-type zeolite is used for the purification of natural gasses including CO<sub>2</sub> [3]. The function of molecular sieves depends on both the pore structure of the zeolite crystal and the conformation of molecule

absorbed [4,5]. Furthermore, Nakazaki et al. [6] have studied the dynamic of the CO<sub>2</sub> molecule in Na-A, MFI-type silicate, mordenite, and X-type and Y-type zeolites by means of computational methods. They reported that X-type zeolite, in particular, is a good adsorbent to CO<sub>2</sub>. Therefore, the present study focused on X-type zeolites for CO<sub>2</sub> adsorption. In this paper, relationships between the CO<sub>2</sub> molecule and alkali ion-exchanged X-type zeolites were studied through computer simulations applying molecular dynamics (MD) and Monte Carlo (MC) methods.

## 2. Method

The cation distribution in X-type zeolites has been widely studied by X-ray diffraction methods [7–9]. The Li-X have proved hard to characterize due to the negligible X-ray scattering power of

\* Corresponding author.

this cation. Often Li-X zeolites contain a combination of both Li and Na cations. A literature search produced four such structures [10–12], and from these anhydrous, Li cation was chosen (form only determined by neutron diffraction) [12].

Dynamic behaviors of CO<sub>2</sub> molecules inside the pores of alkali cation-exchanged X-type zeolites were simulated by applying IMPULSE MD calculation method. The initial velocities of the carbon dioxide molecule was from 750 to 2400 m/s.

The grand canonical ensemble MC simulation technique was used to study the adsorption of CO<sub>2</sub> on zeolites. The MC simulations were performed at 300 K for 1 million steps.

The potential energies between CO<sub>2</sub> and zeolite were calculated applying the Dreiding force field [13].

The results of the calculations were then visualized by computer graphics. The PolyGraf and the CERIOUS software (Molecular Simulation Inc.) were applied for IMPULSE MD and MC calculations, respectively. A graphic super mini-computer TITAN 3000V (Kubota Computer Inc.) was used.

### 3. Results and discussion

#### 3.1. Dynamic behavior of the CO<sub>2</sub> molecule inside the pores of Li-X, Na-X, and K-X

Carbon dioxide molecules having an initial velocity of 1100 m/s cannot pass through the pore of K-X, as shown in Fig. 1. In this figure, X-type zeolite is drawn in the wire frame model. The carbon dioxide molecule and alkali ions in X-type zeolite are shown in the space filling model. The carbon dioxide molecule stays in the super cage of K-X. This figure shows that the CO<sub>2</sub> molecule is absorbed in this position, where the interaction energy between the CO<sub>2</sub> molecule and K-X was –98 kcal/mol. These values become large with increasing initial velocities of the CO<sub>2</sub> molecule.

On the other hand, a CO<sub>2</sub> molecule which has an initial velocity of 2100 m/s can pass through the pores of K-X as shown in Fig. 2. The carbon dioxide molecule diffused inside the pores of K-X while it was colliding with the pore walls. Thereafter it stayed in a super cage of this zeolites for a while, before passing through the pore.

In the case of Na-X, the CO<sub>2</sub> molecule cannot pass through the pore channel of Na-X with initial

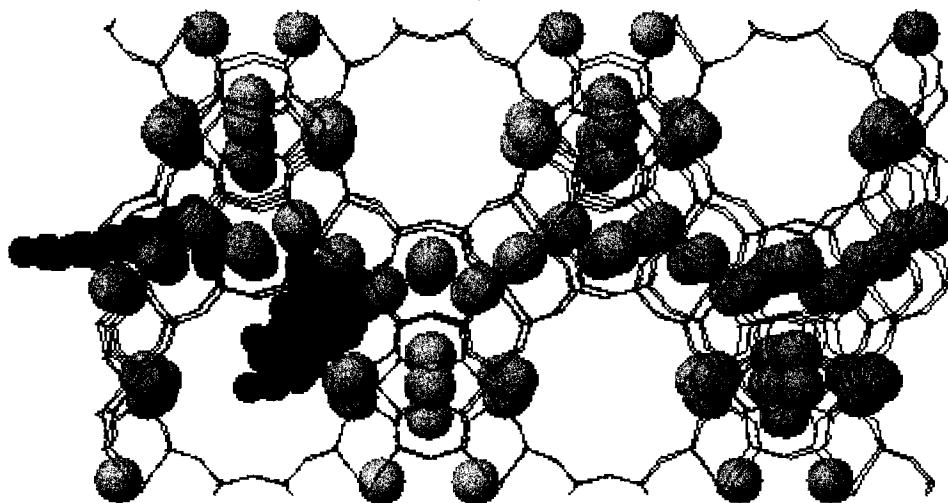


Fig. 1. Dynamic behavior of CO<sub>2</sub> molecule along the pore channel of K-X. Initial velocity of CO<sub>2</sub>, 1100 m/s.

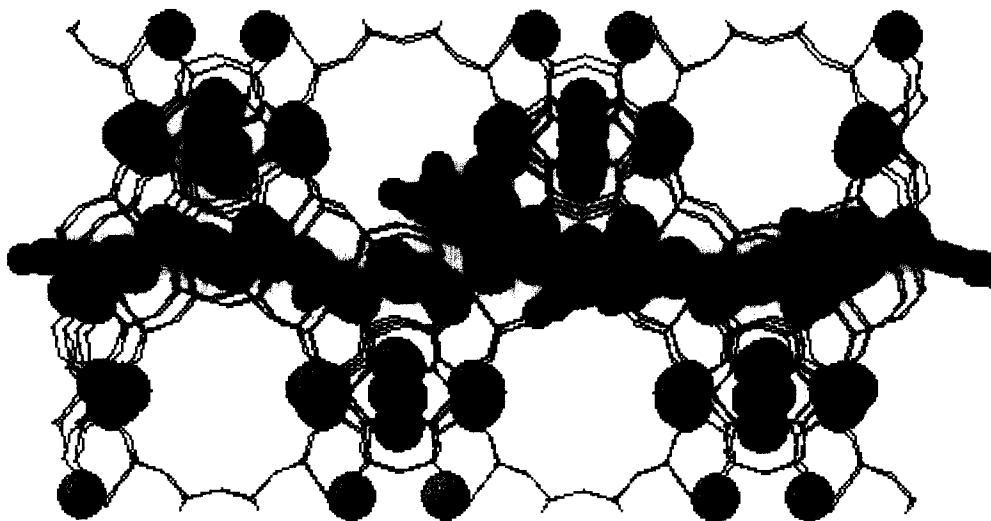


Fig. 2. Dynamic behavior of CO<sub>2</sub> molecule along the pore channel of K-X. Initial velocity of CO<sub>2</sub>, 2100 m/s.

velocities from 1100 to 1850 m/s, because CO<sub>2</sub> collides with the pore walls and is adsorbed.

However, a carbon dioxide molecule which has an initial velocity of more than 2000 m/s can pass through the pore. There are a few differences in the behavior of CO<sub>2</sub> molecules inside the pores of K-X and Na-X. Carbon dioxide was adsorbed in almost the same positions of K-X.

Remarkable results were obtained from MD calculations for Li-X. The carbon dioxide molecule could not pass through the pore channel of Li-X even with an initial velocity of 2400 m/s, because it collided with the pore walls and was adsorbed.

Figs. 3 and 4 show that the CO<sub>2</sub> molecule with initial velocities of 1300 and 2400 m/s stayed near the 3B site of the Li<sup>+</sup> ion in the super cage of Li-X. Inside the pore of Li-X, the electrostatic potential energy term was  $-570$  kcal/mol. This value was very much smaller than those of CO<sub>2</sub> inside the pore of Na-X and K-X. This figure suggested that the CO<sub>2</sub> molecule is adsorbed near the 3B sites of the Li<sup>+</sup> ion in the super cage of Li-X.

### 3.2. Absorption sites of the CO<sub>2</sub> molecule on Li-X, Na-X, and K-X

The MC method, as used during the sorption simulation, randomly creates new trial configurations.

It is thus necessary to effectively fill the free volume of any sites that would be inaccessible in real systems due to small channel windows in the zeolite. In this study, eight additional uncharged dummy atoms were placed in the small sodalite-type cages. This ensures that adsorbates are excluded from these locations during any sorption simulation.

Loading molecules per unit cell of Li-, Na-, and K-X are summarized in Table 1. The ratios of adsorbed CO<sub>2</sub> on Li-X to Na-X and K-X are predicted to be 1.02 and 1.08, respectively. This is due to the sizes of alkali ions inside the pores of X-type zeolites.

A completely random position and orientation of CO<sub>2</sub> molecules were generated. Then configurations having very high energies were rejected, which would almost certainly have been rejected by the next stage of the algorithm. After the CO<sub>2</sub>-framework interaction energy was evaluated, the new configuration was either accepted or rejected. These three steps constitute one step of the simulation. One million steps of this simulation were carried out. The largest amount of adsorbed CO<sub>2</sub> occurs for the case of Li-X. The number of CO<sub>2</sub> molecules absorbed on Li-X in Table 2, 373108, is larger than those of Na-X and K-X. There are strong interactions between CO<sub>2</sub> and zeolites as

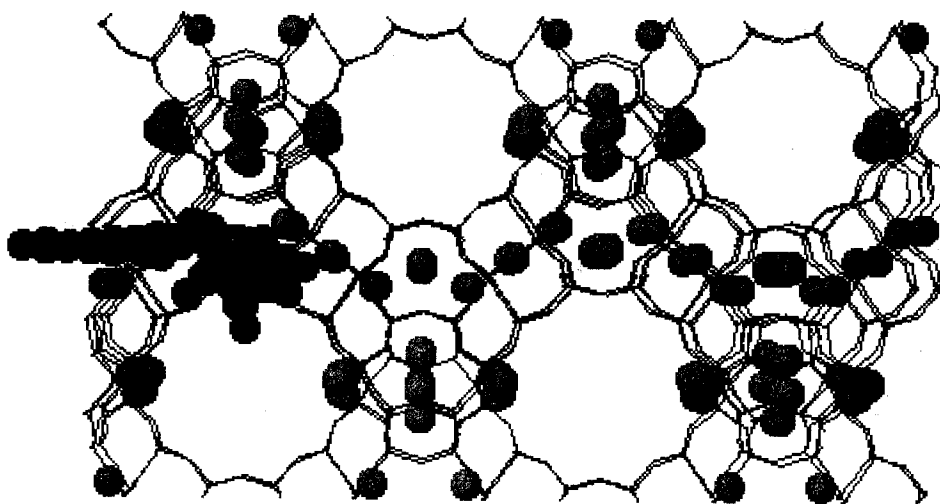


Fig. 3. Dynamic behavior of CO<sub>2</sub> molecule along the pore channel of Li-X. Initial velocity of CO<sub>2</sub>, 1300 m/s.

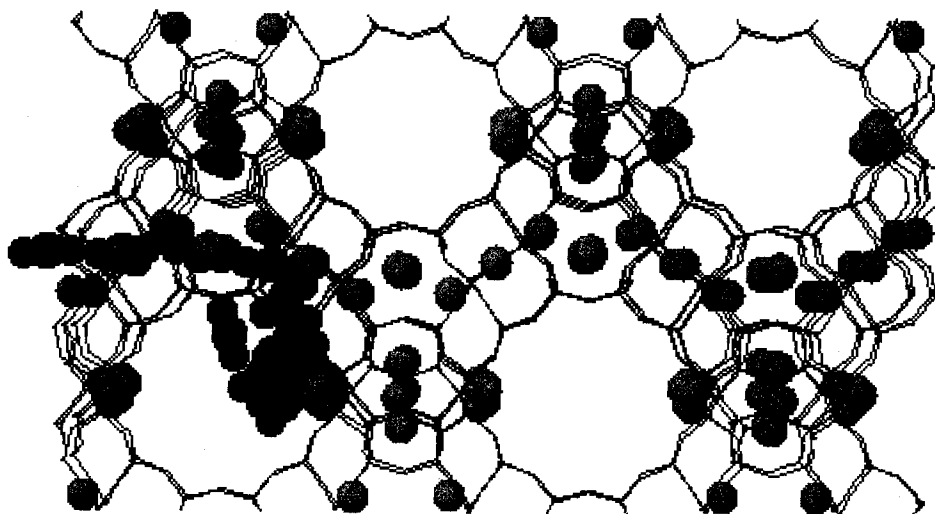


Fig. 4. Dynamic behaviors of CO<sub>2</sub> molecule along the pore channel of Li-X. Initial velocity of CO<sub>2</sub>, 2100 m/s.

Table 1  
Mean loading of CO<sub>2</sub> molecules per unit cell of alkali ion-exchanged X-type zeolites

Zeolite	Mean loading of CO <sub>2</sub> molecule (molecules/unit cell)
Li-X	74.62
Na-X	73.25
K-X	69.03

listed in Table 2. This is due to the greater interaction of the large electrostatics on the CO<sub>2</sub> mol-

ecule with the Li cations. Furthermore, point charges of alkali cations in X-type zeolites, applying the method of Mayo et al. [14], were assigned to the zeolite framework as follows: Li<sup>+</sup> (+1.09), Na<sup>+</sup> (+0.95) and K<sup>+</sup> (+0.83). From these values, it is possible to conclude that the CO<sub>2</sub> molecule has a strong interaction with Li cation in Li-X.

The interaction energies between the CO<sub>2</sub> molecule and alkali ion-exchanged X-type zeolites are shown in Fig. 5. Each curve has a sharp potential

Table 2

Averaged interaction energies between CO<sub>2</sub> molecule and alkali ion-exchanged X-type zeolites

Zeolite	Averaged interaction energy (kcal/mol)	Number of absorbed CO <sub>2</sub> molecules
Li-X	−11.20	373108
Na-X	−10.49	366234
K-X	−9.92	345160

peak at about  $-10$  kcal/mol. The curve of interaction energy between CO<sub>2</sub> molecule and Li-X is broad and exhibits a high interaction energy tail. The CO<sub>2</sub> adsorption energy in the super cage of Li-X is lower than in Na-X and K-X. Therefore, CO<sub>2</sub> is strongly absorbed on the pore walls of Li-X.

Fig. 6a–c shows the predicted mass density plots for CO<sub>2</sub> molecules adsorbed in alkali ion-exchanged X-type zeolites at four atmospheres and 300 K overlaid onto Li-X, Na-X and K-X. These plots show that the CO<sub>2</sub> may occupy all sites within the main cavities but not the small sodalite-type cages from which the adsorbates were excluded by the presence of the blocking atoms. Further the CO<sub>2</sub> molecules exhibit considerable localization. There is no evidence of the distribution remaining diffuse throughout. The dots in these figures represent the center of masses of the successful configuration-averaged random creations produced by the MC algorithm. This shows not only the relationship between the adsorbate and the zeolite cavities, but also the relationship between the localization of the CO<sub>2</sub>

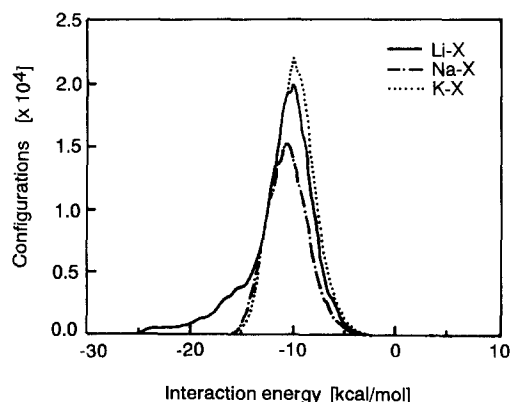


Fig. 5. Calculation adsorption energies of CO<sub>2</sub> in Li-X, Na-X, and K-X

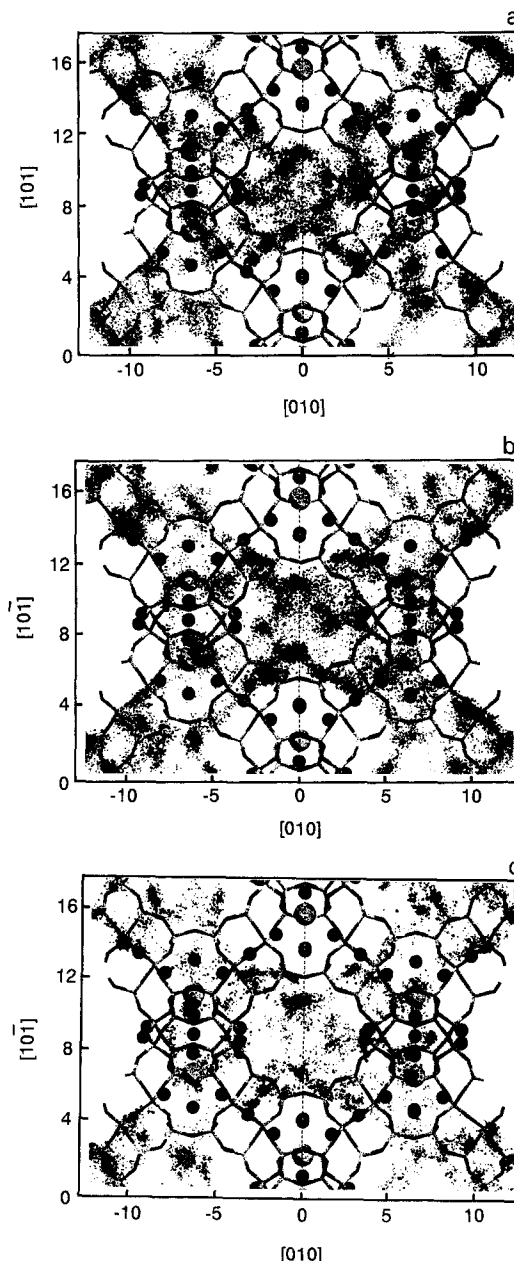


Fig. 6. Mass density plots for CO<sub>2</sub> molecule adsorbed in alkali ion-exchanged X-type zeolites (four atmosphere pressure and 300 K). (a) K-X; (b) Na-X; (c) Li-X.

molecules and the alkali cation positions, shown as spheres.

Fig. 6a shows CO<sub>2</sub> adsorption sites' distribution inside the pore of K-X. As shown in Fig. 6a, carbon dioxide molecules are adsorbed uniformly inside the pore of K-X. The adsorption sites are distributed more uniformly than in the case of Na-X.

The carbon dioxide molecule adsorption sites' distribution inside the pore of Na-X is shown in Fig. 6b. This figure shows that the adsorption sites of the CO<sub>2</sub> molecule are distributed uniformly inside the pores of Na-X.

On the other hand, Fig. 6c shows CO<sub>2</sub> adsorption sites' distribution inside the pores of Li-X. The dots concentrated specific areas inside the super cage of Li-X. This indicated that the CO<sub>2</sub> molecule would be adsorbed strongly near the 3B site of the Li<sup>+</sup> ion.

#### 4. Conclusion

Li-X is shown from this study to be a good adsorbate from every point of view, i.e. MD calculation results, sizes and point charges of alkali cations, and MC simulation.

Molecular dynamics and Monte Carlo simulation provide a useful technique for the determination of CO<sub>2</sub> adsorption on zeolites. The present study focused on X-type zeolites for CO<sub>2</sub> adsorp-

tion. However, the method used here is applicable to a wide range of adsorption-based gas separation processes. The approach can provide understanding of the factors influencing gas separation properties which can be used to design superior gas separation adsorbents and to optimize operating conditions for separation process.

#### References

- [1] T. Inui, Y. Okugawa and M. Yasuda, *Ind. Eng. Chem. Res.*, 27 (1988) 1103.
- [2] T. Inui, M. Shibata, W. Tanakulrungsank and T. Takeguchi, *Gas Separation and Purification*, 6 (1992) 185.
- [3] P.A. Jacobs and R.A. van Santen (Editors), *Zeolites: Facts, Figures, Future*, (Stud. Surf. Sci. Catal., Vol. 49, Parts A and B), Elsevier, Amsterdam, 1989.
- [4] T. Inui and Y. Nakazaki, *Zeolites*, 11 (1991) 434.
- [5] Y. Nakazaki, N. Goto and T. Inui, *J. Catal.*, 136 (1992) 141.
- [6] Y. Nakazaki, Y. Tanaka, N. Goto and T. Inui, *Abstract of TOCAT2*, (1994) P096.
- [7] W.J. Mortier, *Compilation of Extra-framework Sites in Zeolites*, Butterworth, London, 1982.
- [8] R. Schollner, R. Broddack, B. Kuhlmann, P. Nozel and H.Z. Herden, *Phys. Chem.*, 262 (1981) 17.
- [9] T.S. Egerton and F.S.J. Stone, *J. Chem. Soc., Faraday Trans. 1*, 66 (1970) 2364.
- [10] H. Herden, W.D. Einicke, R. Schoellner, W.J. Mortier, L.R. Gellens and J.B. Uytterhorven, *Zeolites*, 2 (1982) 131.
- [11] Y.F. Shepelev, A.A. Anderson and Y.I. Smith, *Zeolites*, 10 (1990) 61.
- [12] C. Forano, R.C.T. Slade, E.K. Anderson, E.G. Anderson and E. Prince, *Solid State Chem.*, 82 (1989) 95.
- [13] S. Dasgupta and W.A. Goddard III, *J. Phys. Chem.*, 90 (1989) 7207.
- [14] S.L. Mayo, B.D. Olfson and W.A. Goddard III, *J. Phys. Chem.*, 94 (1990) 8897.